

## Supporting information

### Distribution Coefficients of the REEs, Sr, Y, Ba, Th, and U between $\alpha$ -HIBA and AG50W-X8 Resin

Haoyu Li<sup>1</sup>, François L. H. Tissot<sup>1,2\*</sup>, Seung-Gu Lee<sup>2,3</sup>, Eugenia Hyung<sup>1</sup>, and Nicolas Dauphas<sup>2</sup>

<sup>1</sup>The Isotoparium, Division of Geological and Planetary Sciences, California Institute of Technology, Pasadena 91125, California, United States.

<sup>2</sup>Origins Laboratory, Department of the Geophysical Sciences and Enrico Fermi Institute, The University of Chicago, Chicago, Illinois 60637, USA.

<sup>3</sup>Geological Research Division, Korea Institute of Geoscience and Mineral Resources, Daejeon 34132, Republic of Korea

#### Table of contents

- Appendix. Estimation of  $^{141}\text{Pr}^{16}\text{O}$  interference on  $^{157}\text{Gd}$ .
- Table S1. Architecture of the chromatography simulation code.
- Figure S1. Results of simulated elution obtained using various column dimensions.
- Figure S2. Results of simulated elution obtained using various resin properties.
- Figure S3. The 95% confidence intervals of best-fit linear regression lines for determination of REE  $K_d$  as a function of  $\alpha$ -HIBA molarity.

### Estimation of $^{141}\text{Pr}^{16}\text{O}$ interference on $^{157}\text{Gd}$ .

Below, we present derivations of the influence of  $^{141}\text{Pr}^{16}\text{O}$  interference on the  $K_d$  determination of  $^{157}\text{Gd}$ . By definition, the distribution coefficient is the ratio of the concentration of an element of interest in the immobile phases (here the resin) over the concentration in the mobile phase (here the  $\alpha$ -HIBA solution. Therefore, the  $K_{d,s}$  for Pr and Gd can be expressed as (after simplifying for volume and weight of resin):

$$K_d^{\text{Pr}} = \frac{[\text{Pr}]_b - [\text{Pr}]_a}{[\text{Pr}]_a} \quad (\text{S.1})$$

$$K_d^{\text{Gd}} = \frac{[\text{Gd}]_b - [\text{Gd}]_a}{[\text{Gd}]_a} \quad (\text{S.2})$$

where the subscript  $a$  and  $b$  refer to before and after resin-liquid equilibration.

In the presence of a PrO interference, the measured (subscript  $m$ )  $K_d$  of Gd can be expressed as:

$$K_d^{\text{Gd}_m} = \frac{([\text{Gd}]_b + [\text{PrO}]_b) - ([\text{Gd}]_a + [\text{PrO}]_a)}{([\text{Gd}]_a + [\text{PrO}]_a)} = \frac{([\text{Gd}]_b + [\text{Pr}]_b f) - ([\text{Gd}]_a + [\text{Pr}]_a f)}{([\text{Gd}]_a + [\text{Pr}]_a f)} \quad (\text{S.3})$$

where  $f$  is the fraction of oxidized Pr detected at mass 157.

From the Eq. (S.2), the Gd concentration before equilibration is:

$$[\text{Gd}]_b = (K_d^{\text{Gd}} + 1) [\text{Gd}]_a \quad (\text{S.4})$$

Substituting Eq. (S.4) into Eq. (S.3), one obtains that

$$K_d^{\text{Gd}_m} = \frac{((K_d^{\text{Gd}} + 1) [\text{Gd}]_a + [\text{Pr}]_b f) - ([\text{Gd}]_a + [\text{Pr}]_a f)}{([\text{Gd}]_a + [\text{Pr}]_a f)} \quad (\text{S.5})$$

To estimate  $f$  (the oxide production rate for Pr) in these equations, and based on the measured  $K_d$  values (Table 2), we can assume that  $10K_d^{\text{Gd}_m} \approx K_d^{\text{Pr}}$ , and therefore:

$$[\text{Pr}]_b = (K_d^{\text{Pr}} + 1)[\text{Pr}]_a \approx (10K_d^{\text{Gd}_m} + 1)[\text{Pr}]_a \quad (\text{S.6})$$

Given that the concentration of Pr and Gd before the equilibration were the same in the batch experiments solution, after equilibration, the concentration of Gd in the liquid will be about 10 times higher than that of Pr (*i.e.*,  $[\text{Gd}] = 10 [\text{Pr}]$ , since  $10K_d^{\text{Gd}_m} \approx K_d^{\text{Pr}}$ ). The measured and actual concentration of Gd in the liquid before and after equilibration can thus be written as:

$$[\text{Gd}] = [\text{Gd}]_m - [\text{Pr}]f \approx (10 - f)[\text{Pr}] \quad (\text{S.7})$$

Substituting Eq. (S.7) into Eq. (S.5) yield the  $K_d^{\text{Gd}}$  corrected for PrO interferences as:

$$K_d^{\text{Gd}} \approx K_d^{\text{Gd}_m} - \frac{9K_d^{\text{Gd}_m} \times f}{(10 - f)} \quad (\text{S.8})$$

The fraction of Pr oxidized is thus equal to:

$$f = \frac{10(K_d^{\text{Gd}_m} - K_d^{\text{Gd}})}{(10K_d^{\text{Gd}_m} - K_d^{\text{Gd}})} \quad (\text{S.9})$$

Considering  $^{141}\text{Pr}$  and  $^{157}\text{Gd}$  were the measured isotopes during the mass spectrometry, the abundance of  $^{157}\text{Gd}$  ( $A_{157} = 15.65\%$ ) and  $^{141}\text{Pr}$  ( $A_{141} = 100\%$ ) should be taken into account during the derivation, which yields:

$$f = \frac{10(K_d^{\text{Gd}_m} - K_d^{\text{Gd}})}{(10K_d^{\text{Gd}_m} - K_d^{\text{Gd}})} \times \frac{A_{157}}{A_{141}} \quad (\text{S.10})$$

If using the corrected slope and intercept of Gd (Fig. 2 and Table 3) to calculate the actual  $K_d$  of Gd, the  $f$  in Eq. (S.12) is approximately 10%, which is a typical oxide production rate for MC-ICPMS with the spray chamber, supporting the need for the correction of the  $K_d$  values for Gd, as done in the main text.

**Table S1.** Architecture of the chromatography simulation code

---

1) Set collection volume of the elution scheme	
2) Import resin characteristics:	HETP (cm), Column height (cm), Column radius (cm), Resin porosity, Density of extractant-loaded beads (g/mL).
3) Import elution details:	Number of elution steps, Volume of each elution step (mL), Element concentration in each elution step (mol/mL), $K_d$ of elements in each elution step.
4) Elution simulation loop	
	For each elution step:
	<ul style="list-style-type: none"><li>• The characteristics of the liquid volume to inject are updated,</li><li>• The liquid in the last plate is eluted,</li><li>• The liquid in each plate above the last one is moved down one plate,</li><li>• The liquid to inject is added to the first plate,</li><li>• Liquid-solid equilibrium is calculated in each plate.</li></ul>
End of the loop	
Plot the simulated elution curve (% recovery vs. volume). Two graphs are plotted, in the first one, the volume step is the plate column, in the second one it is the collection volume specified by the user.	
Export the results as xls or xlsx file.	

---

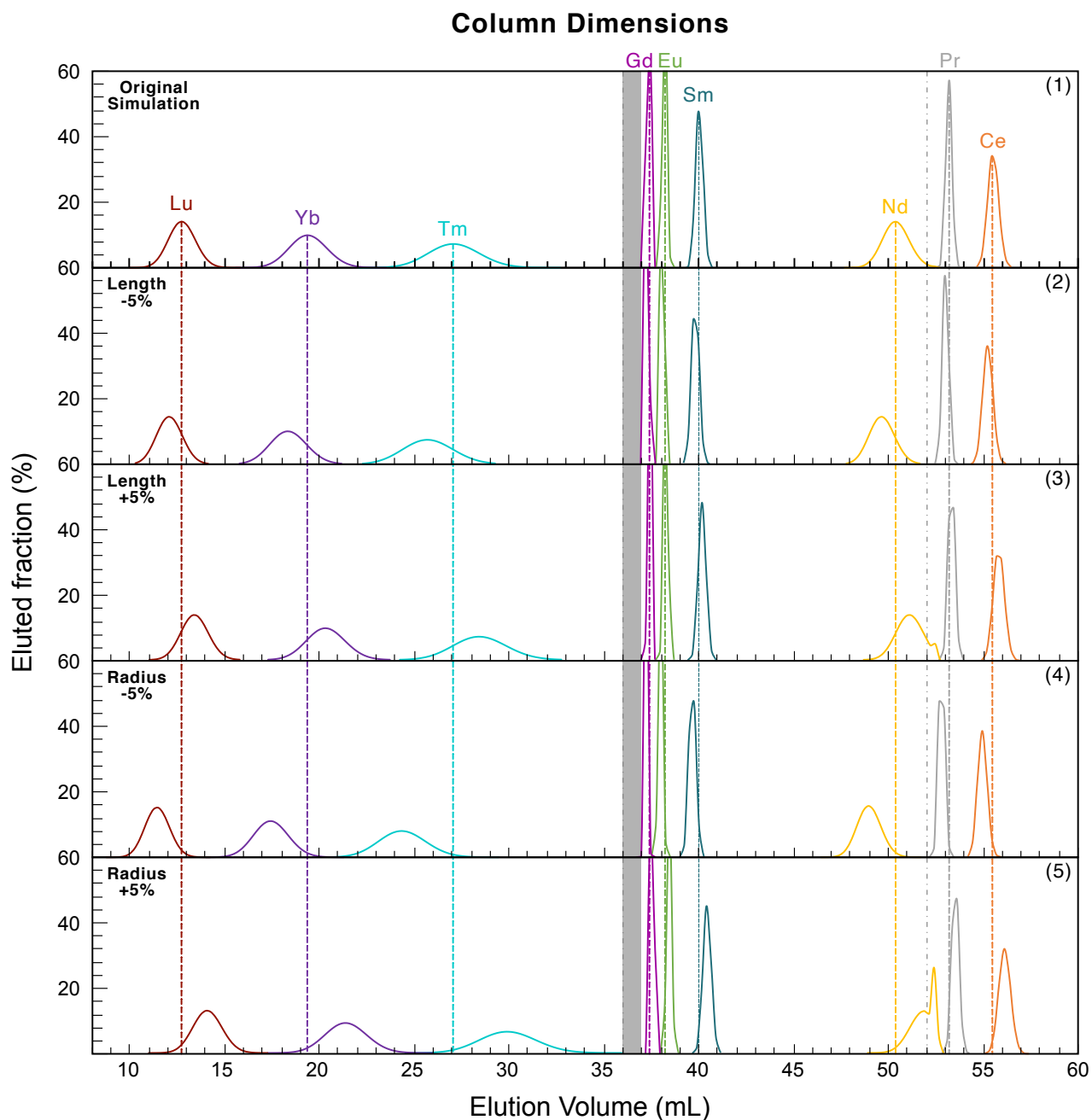


**Figure S1.** Sensitivity tests for the elution simulations depending on column dimensions. Panel (1) shows the original simulation (collected volume = 0.25 mL); while panels (2)-(5) shows the labeled parameters changed by  $\pm 5\%$ , while keeping other parameters constant. The grey dot dash lines represent the transitions of  $\alpha$ -HIBA molarity, and the dash lines represent the positions of peaks in the original simulated elution profile. The grey band denotes the position of elution of Er, Ho, Dy and Tb, whose simulations do not change with input parameters.

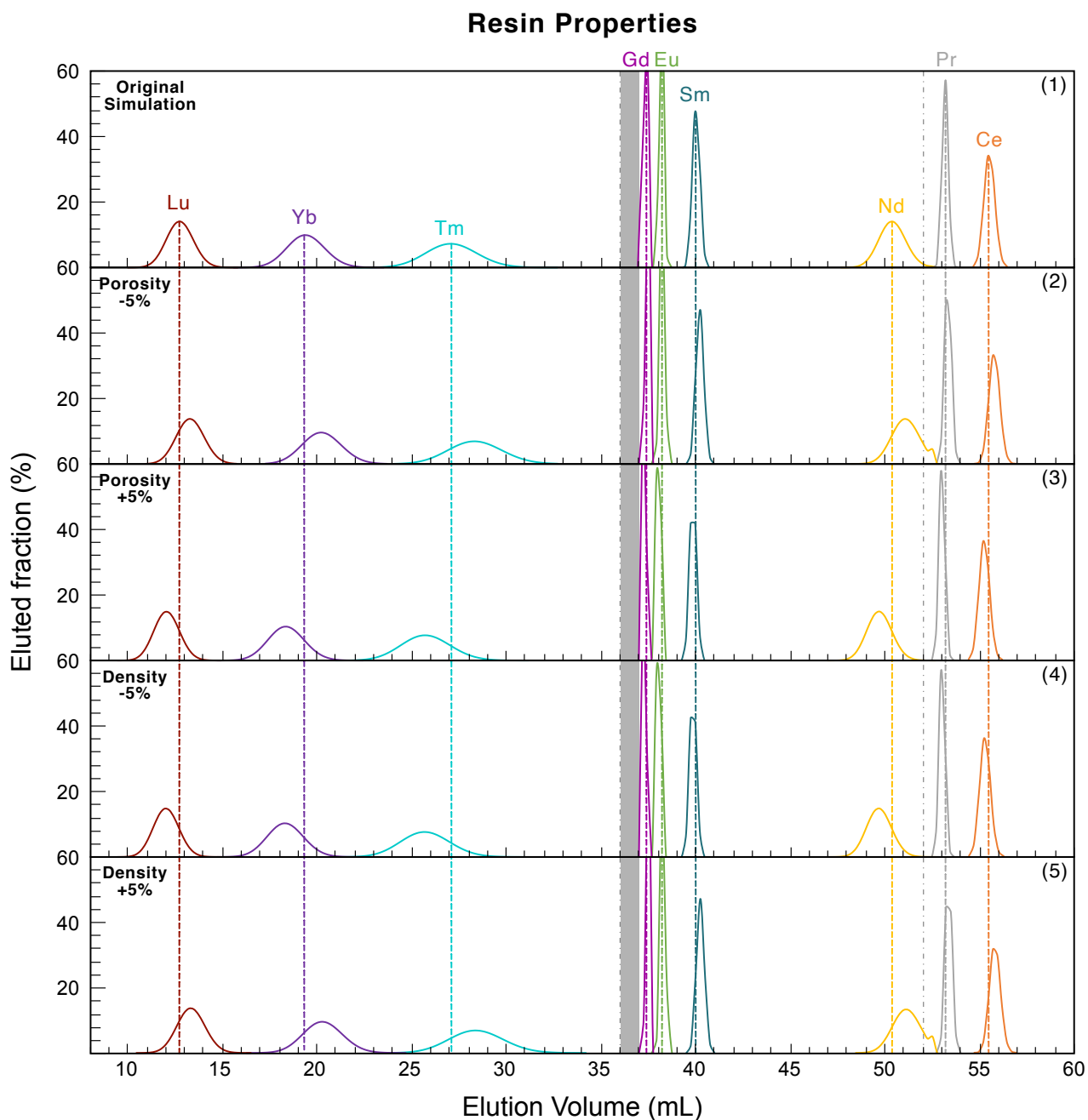


**Figure S2.** Sensitivity tests for the elution simulations depending on resin properties. Panel (1) shows the original simulation (collected volume = 0.25 mL); while panels (2)-(5) shows the labeled parameters changed by +/- 5%, while keeping other parameters constant. The grey dot dash lines represent the transitions of  $\alpha$ -HIBA molarity, and the dash lines represent the positions of peaks in the original simulated elution profile. The grey band denotes the position of elution of Er, Ho, Dy and Tb, whose simulations do not change with input parameters.

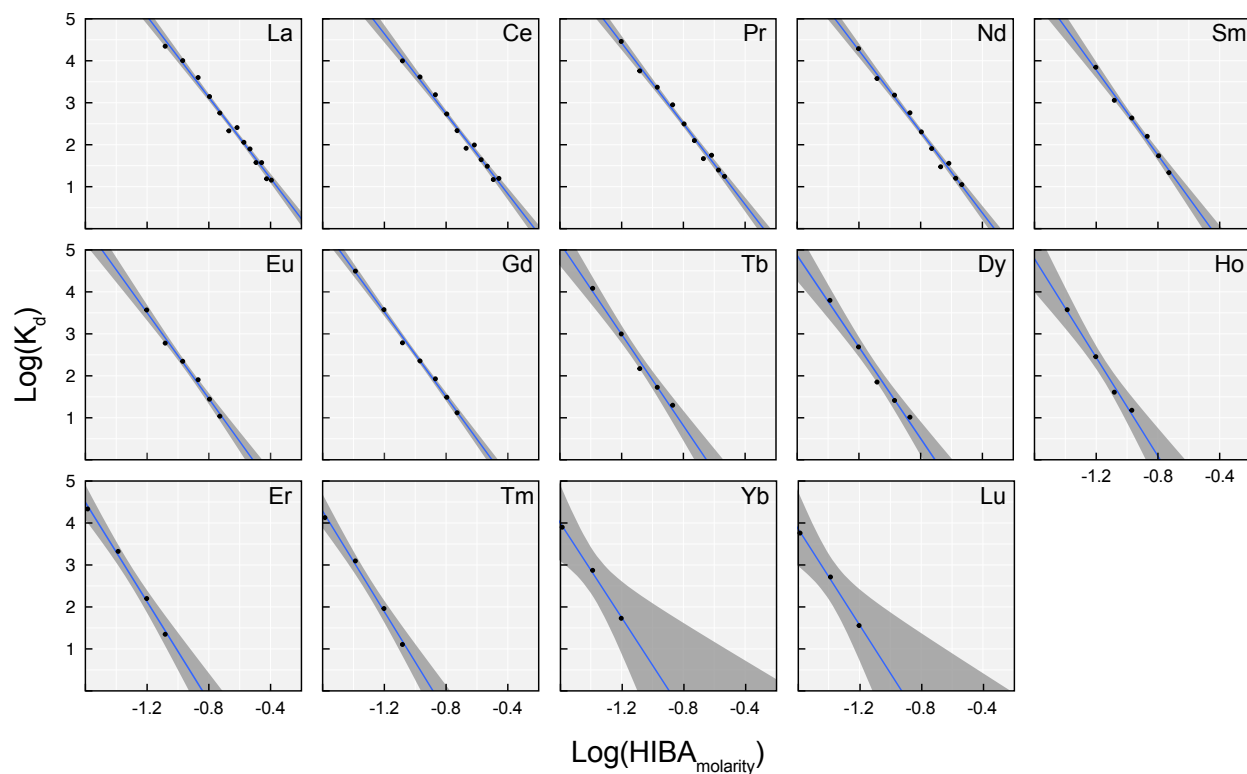


**Figure S3.** The 95% confidence intervals of best-fit linear regression lines for determination of REE  $K_d$  as a function of  $\alpha$ -HIBA molarity. Black points= measured  $K_d$  values at given  $\alpha$ -HIBA molarities; blue lines= best-fit linear regression lines; dark grey band= 95% confidence intervals.